

Relevance of the axial anomaly at the finite-temperature chiral transition in QCD

Andrea Pelissetto

Dipartimento di Fisica dell'Università di Roma "La Sapienza" and INFN, Sezione di Roma I, I-00185 Roma, Italy

Ettore Vicari

Dipartimento di Fisica dell'Università di Pisa and INFN, Sezione di Pisa, I-56127 Pisa, Italy

(Dated: November 11, 2013)

We investigate the nature of the finite-temperature chiral transition in QCD with two light flavors, in the case of an effective suppression of the $U(1)_A$ symmetry breaking induced by the axial anomaly, which implies the symmetry breaking $U(2)_L \otimes U(2)_R \rightarrow U(2)_V$, instead of $SU(2)_L \otimes SU(2)_R \rightarrow SU(2)_V$. For this purpose, we perform a high-order field-theoretical perturbative study of the renormalization-group flow of the corresponding three-dimensional multiparameter Landau-Ginzburg-Wilson Φ^4 theory with the same symmetry-breaking pattern. We confirm the existence of a stable fixed point, and determine its attraction domain in the space of the bare quartic parameters. Therefore, the chiral QCD transition might be continuous also if the $U(1)_A$ symmetry is effectively restored at T_c . However, the corresponding universality class differs from the $O(4)$ vector universality class which would describe a continuous transition in the presence of a substantial $U(1)_A$ symmetry breaking at T_c . We estimate the critical exponents of the $U(2)_L \otimes U(2)_R \rightarrow U(2)_V$ universality class by computing and analyzing the corresponding perturbative expansions. These results are important to discriminate among the different scenarios for the scaling behavior of QCD with two light flavors close to the chiral transition.

PACS numbers: 12.38.Aw, 25.75.Nq, 11.10.Wx, 11.30.Rd, 05.10.Cc

I. INTRODUCTION

At finite temperature (T) nuclear matter shows two different phases: a low- T hadronic phase, in which chiral symmetry is broken, and a high- T phase, in which chiral symmetry is restored and quarks and gluons are unbounded [1–6]. Since the u and d quarks are very light, a great amount of work has been devoted to the study of QCD with N_f light flavors, $N_f = 2$ being the physically interesting case. In this limit the QCD Lagrangian is invariant under $U(N_f)_L$ and $U(N_f)_R$ transformations. Since

$$U(N)_{L,R} \cong U(1)_{L,R} \otimes [SU(N)/\mathbb{Z}(N)]_{L,R}, \quad (1)$$

and the group $U(1)_L \otimes U(1)_R$ is isomorphic to the group $U(1)_V \otimes U(1)_A$ of vector and axial $U(1)$ transformations, the classical symmetry group of the theory can be written as

$$U(1)_V \otimes U(1)_A \otimes [SU(N_f)/\mathbb{Z}(N_f)]_L \otimes [SU(N_f)/\mathbb{Z}(N_f)]_R. \quad (2)$$

The vector subgroup $U(1)_V$ corresponds to the quark-number conservation and it is not expected to play any role at the transition. The $U(1)_A$ symmetry is broken to $\mathbb{Z}(N_f)_A$ by quantum fluctuations, since the divergence of the corresponding current presents a quantum anomaly proportional to the topological charge density. This reduces the relevant symmetry to [5]

$$[SU(N_f)_L \otimes SU(N_f)_R]/\mathbb{Z}(N_f)_V. \quad (3)$$

At zero temperature, the hadronic spectrum shows that this symmetry is spontaneously broken to $SU(N_f)_V$ with $N_f^2 - 1$ Goldstone particles (pions and kaons) and a

nonzero quark condensate $\langle \bar{\psi}\psi \rangle$. The large mass difference between the pseudoscalar flavor singlet and nonsinglet mesons, such as η and η' , which have the same quark content, reflects the quantum breaking of the $U(1)_A$ symmetry.

At finite temperature, a phase transition occurs at a critical temperature T_c , $T_c \simeq 160$ MeV for $N_f = 2$. Above T_c , chiral symmetry is restored and the quark condensate vanishes. Therefore, the symmetry-breaking pattern at the chiral transition is expected to be

$$[SU(N_f)_L \otimes SU(N_f)_R]/\mathbb{Z}(N_f)_V \rightarrow SU(N_f)_V/\mathbb{Z}(N_f)_V, \quad (4)$$

with a matrix-like order parameter given by the expectation value of the quark bilinear $\Psi_{ij} \equiv \bar{\psi}_{L,i}\psi_{R,j}$. In the case of two flavors, i.e. $N_f = 2$, the symmetry-breaking pattern (4) is equivalent to that of the $O(4)$ vector model, i.e., to $O(4) \rightarrow O(3)$ [7–15]. Thus, in the case of a continuous transition, the critical behavior of the model with two massless flavors is expected to belong to the three-dimensional (3D) $O(4)$ universality class.

The symmetry-breaking pattern at the transition significantly changes if also the $U(1)_A$ symmetry is restored. The anomaly effects breaking the $U(1)_A$ symmetry are related to the topological properties of QCD. Semiclassical instanton calculations predict a substantial suppression of the instanton density for $T \gg T_c$, where the dilute instanton gas (DIG) model is expected to provide a reliable approximation [16]. For example, in QCD with N_f light flavors of mass m , the topological susceptibility χ is expected to decay asymptotically as [16]

$$\chi \sim m^{N_f} T^{-\kappa}, \quad \kappa = \frac{11}{3}N_c + \frac{1}{3}N_f - 4 \quad (5)$$

where N_c is the number of colors. For $N_c = 3$ and $N_f = 2$ we have $\kappa = 23/3$. Although χ vanishes in the massless limit, the Dirac zero modes associated with the instantons induce a residual contribution to the $U(1)_A$ symmetry breaking, giving rise to a difference between the susceptibilities of the so-called π and δ channels at high T [17, 18], which behaves as $\chi_\pi - \chi_\delta \sim T^{-\kappa}$ in the chiral massless limit.

The breaking of the $U(1)_A$ symmetry at finite T , and its role at the chiral transition, has been much investigated [17–34]. Monte Carlo (MC) simulations of lattice QCD [17–25] find a substantial suppression of the $U(1)_A$ anomaly effects at large T , as predicted by the DIG model. These results are supported by numerical investigations of pure $SU(N)$ gauge theories, which show that the topological susceptibility is rapidly suppressed above the deconfinement transition, see, e.g., Ref. [35] and references therein, and that the DIG regime sets in quite early for $T \gtrsim T_c$ [36]. There are also some claims of an exact restoration of the $U(1)_A$ symmetry at the chiral transition [20, 21].

It is thus worth investigating the nature of the finite- T chiral transition in the case the $U(1)_A$ symmetry is effectively restored, and the relevant symmetry-breaking pattern is

$$[U(N_f)_L \otimes U(N_f)_R]/U(1)_V \rightarrow U(N_f)_V/U(1)_V, \quad (6)$$

instead of that reported in Eq. (4).

Up to now we have discussed the case of the model with N_f massless flavors. However, in nature quarks have a finite mass. Since u and d quarks are very light, one expects that the correct physical behavior can be obtained by considering their masses as a perturbation in the theory with $N_f = 2$. According to renormalization-group (RG) theory, if the transition is continuous in the chiral massless limit, then an analytic crossover is expected for nonzero values of the quark masses m_f , because the quark masses act as external fields coupled to the order parameter. Still, the presence of a close continuous transition gives rise to scaling relations depending on the fermion mass $m_f = m$ and on the reduced temperature $t \equiv (T - T_c)/T_c$. For instance, the fermion condensate is expected to scale as

$$\langle \bar{\psi}\psi \rangle \propto m^{1/\delta} E(m^{-1/(\beta+\gamma)}t), \quad (7)$$

where δ , β and γ are appropriate critical exponents determined by the universality class of the transition, see e.g. Refs. [7, 37–39], and $E(x)$ is an universal scaling function (apart from trivial normalizations). On the other hand, a first-order transition is generally robust against perturbations. Therefore, if the massless theory undergoes a first-order transition, we expect a first-order transition also for small nonvanishing values of the masses, up to an endpoint m^* , around which a 3D Ising critical behavior is expected. For larger fermion masses the phase transition disappears and we have an analytic crossover as well.

To make contact with experiments, it is also necessary to take into account the massive strange quark s , whose

mass ($m_s \approx 100$ MeV) is comparable with T_c . Since the transition is expected to be of first order for $N_f = 3$ light degenerate quarks, we also expect a first-order transition when increasing m_s (keeping $m_u = m_d = 0$), at least for sufficiently small values of m_s . For larger values of m_s there are two possibilities, depending on the nature of the transition for $N_f = 2$ degenerate quarks, corresponding to the limit $m_s \rightarrow \infty$. In one case we may have a first-order transition line which extends for all values of m_s . Alternatively, the first-order transition line extends up to a finite m_s^* , then the transition becomes continuous for $m_s > m_s^*$, and in particular in the limit $m_s \rightarrow \infty$; m_s^* is a tricritical point, separating the first-order transition line from the critical line, which implies that the critical behavior for $m_s = m_s^*$ should be described by mean-field theory, with logarithmic corrections.

The nature of the chiral transition has been extensively studied. In spite of several MC studies of different lattice QCD formulations with two light quarks [40–50], the nature of the chiral transition is still controversial. Some MC results favor a continuous transition, but are not sufficiently accurate to clearly identify the corresponding universality class. Other MC studies report instead evidence of a first-order transition. For quark masses close to their physical values, the results of MC simulations [51–58] support a crossover scenario: the low- T and high- T regimes are not separated by a phase transition, but rather by a crossover region in which the thermodynamic quantities change rapidly, but continuously, in a relatively narrow temperature interval.

The universal features of the chiral transition can be investigated within the RG framework [37, 38]. They are determined by a few global properties, such as the space dimensionality d ($d = 3$ for the finite- T QCD transition), the nature and the symmetry of the order parameter (a complex matrix related to the bilinear quark operators $\bar{\psi}_{Li}\psi_{Rj}$), and the symmetry-breaking pattern (which is given by Eqs. (4) or (6) depending on the role played by the $U(1)_A$ anomaly). For this purpose one considers the RG flow in the space of Lagrangians which satisfy the above-reported general properties and determines the fixed points (FPs) of the flow. In the absence of a stable FP, only first-order transitions between the disordered and ordered phases are possible. On the other hand, if a stable FP exists, the transition may be continuous, and the usual critical exponents ν , η , etc... are related to the eigenvalues of the linearized flow around the FP. However, it is important to stress that, even in the presence of a stable FP, some systems may still undergo a first-order transition. From the RG point of view, this occurs in systems which are not in the attraction domain of the stable FP.

To determine the RG behavior of the model, one can use standard perturbative field-theoretical approaches [7, 39]. The first RG study of the effective model with symmetry-breaking pattern (6) was presented by Pisarski and Wilczek [5], who performed a one-loop calculation within the ϵ expansion, $\epsilon = 4 - d$, finding no stable FP

TABLE I: Summary of the RG predictions for the finite- T QCD transition, as a function of the number N_f of light flavors. We distinguish two cases, depending whether the $U(1)_A$ symmetry is broken or effectively restored. When a continuous transition is possible, we specify the corresponding 3D universality class by reporting its symmetry-breaking pattern.

N_f	$U(1)_A$ broken	$U(1)_A$ restored
1	crossover or 1 st ord	$O(2) \rightarrow \mathbb{Z}_2$ or 1 st ord
2	$O(4) \rightarrow O(3)$ or 1 st ord	$U(2)_L \otimes U(2)_R \rightarrow U(2)_V$ or 1 st ord
≥ 3	1 st ord	1 st ord

close to $d = 4$. This result suggests a first-order transition for the model with symmetry-breaking pattern (6). However, subsequent analyses of the RG flow directly in three dimensions, based on high-order perturbative expansions (up to six loops), have provided the evidence of a stable 3D FP [59–61]. Thus, the transition may also be continuous if the $U(1)_A$ symmetry is effectively restored at T_c . However, its universality class differs from the 3D $O(4)$ universality class.

Table I summarizes the results of these RG analyses, reporting the possible transitions for various values of N_f , and for the two symmetry breaking patterns (4) and (6). When a continuous transition is possible, the corresponding universality class is reported.

In this paper we extend previous field-theoretical studies [59–61] of the 3D $U(2)_L \otimes U(2)_R \rightarrow U(2)_V$ universality class. Our purpose is to provide accurate predictions for the critical features of this universality class, for which we know much less compared with the $O(N)$ vector universality classes. We study the RG flow of the multiparameter Φ^4 theory with the same symmetry breaking. For this purpose, we consider two different 3D perturbative schemes: the massive zero-momentum (MZM) scheme [7, 39, 62] and the 3D minimal subtraction scheme \overline{MS} without ϵ expansion [63, 64].

The resummation of the perturbative expansions of the β functions (known to six and five loops in the MZM and \overline{MS} scheme, respectively) allows us to compute the RG trajectories starting from the unstable Gaussian FP of the free theory. They approach a stable FP in both schemes for an extended region of bare parameters. Moreover, we estimate the critical exponents by computing the expansions of appropriate RG functions and evaluating them at the stable FP.

The paper is organized as follows. In Sec. II we review the universality and RG arguments which we use to investigate the finite- T transition in QCD with $N_f = 2$ light flavors. In particular, we define the effective theory that is relevant for the model with symmetry-breaking pattern (6). In Sec. III we study the RG flow in the space of the renormalized couplings; in particular we determine the RG trajectories that start at the unstable Gaussian FP of the free quadratic theory and flow to-

wards the stable FP controlling the critical behavior at the transition. Moreover, we determine the critical exponents by evaluating appropriate RG functions at the stable FP. Finally, in Sec. IV we draw our conclusions. In App. A we report the perturbative expansions used in the paper to determine the RG flow and the critical exponents.

II. RG ANALYSIS OF THE CHIRAL TRANSITION

The nature of the finite- T chiral transition in QCD can be investigated using universality and RG arguments [5, 59–61, 65]. In this section we review them, focussing on the finite- T transition in QCD with two light flavors.

Let us first assume that the phase transition at T_c is continuous for vanishing quark masses. In this case the length scale of the critical modes diverges approaching T_c , becoming eventually much larger than $1/T_c$, which is the size of the euclidean “temporal” dimension at T_c . Therefore, the asymptotic critical behavior is associated with a 3D universality class with the same symmetry breaking pattern and the order parameter is an $N \times N$ complex-matrix field Φ_{ij} , related to the bilinear quark operators $\bar{\psi}_{Li}\psi_{Rj}$. Nonvanishing quark masses can be accounted for by an external field coupled to the order parameter.

To determine the critical behavior we consider the most general Landau-Ginzburg-Wilson (LGW) Φ^4 theory compatible with the given symmetry breaking. If Eq. (6) holds, the theory is given by

$$\mathcal{L}_{U(N)} = \text{Tr}(\partial_\mu \Phi^\dagger)(\partial_\mu \Phi) + r \text{Tr} \Phi^\dagger \Phi + \frac{u_0}{4} (\text{Tr} \Phi^\dagger \Phi)^2 + \frac{v_0}{4} \text{Tr} (\Phi^\dagger \Phi)^2, \quad (8)$$

where the field Φ_{ij} is a generic $N \times N$ complex matrix. The symmetry is $U(N)_L \otimes U(N)_R$, which breaks to $U(N)_V$ if $v_0 > 0$, thus providing the LGW theory relevant for QCD with two light flavors. The reduction of the symmetry to $SU(N)_L \otimes SU(N)_R$ for QCD, due to the axial anomaly, can be achieved by adding additional quadratic and quartic terms containing the determinant of the field Φ [61]. We return to this point later.

The critical behavior at a continuous transition is controlled by the FPs of the RG flow, which are determined by the common zeroes of the β -functions associated with the quartic parameters. To study the RG flow of the Φ^4 theory (8), we consider two different perturbative schemes.

In the massive zero-momentum (MZM) scheme [7, 39, 62] one performs the perturbative expansion directly in three dimensions, in the critical region of the disordered phase. The MZM perturbative expansions of the β functions and of the critical exponents have been computed to six loops, requiring the computation of approximately 1000 Feynman diagrams. The six-loop series of the β functions were reported in Ref. [61], here we also report

those of the RG functions associated with the critical exponents, in App. A 1.

In the 3D $\overline{\text{MS}}$ scheme one considers the massless critical theory: one uses dimensional regularization and the modified minimal-subtraction prescription, thus the RG functions are obtained from the divergences appearing in the perturbative expansion of the correlation functions [66]. In the standard ϵ -expansion scheme [67], the FPs, i.e., the common zeroes of the β -functions, are determined perturbatively as expansions in powers of $\epsilon \equiv d - 4$, while exponents are obtained by expanding the corresponding RG functions computed at the FP in powers of ϵ . Physical results are then obtained by extrapolating the results to $d = 3$. This procedure assumes the existence of a FP for $\epsilon \rightarrow 0$, i.e., close to four dimensions. Therefore, it allows one to determine only those three-dimensional FPs which can be defined, by analytic continuation, close to four dimensions. Other FPs, which do not have a four-dimensional counterpart, cannot be detected. This problem is overcome by the 3D $\overline{\text{MS}}$ scheme without ϵ expansion [63, 64, 68]. The RG functions $\beta_{u,v}$ and $\eta_{\phi,t}$ are the $\overline{\text{MS}}$ functions. However, $\epsilon \equiv 4 - d$ is no longer considered as a small quantity, but it is set equal to its physical value ($\epsilon = 1$ in our case) before computing the FPs. This provides a well defined 3D perturbative scheme which allows us to compute universal quantities, without the need of expanding around $d = 4$ [63, 64]. In the $\overline{\text{MS}}$ scheme the RG series of the β functions are known up to five loops [69]; here we also present the five-loop series of the RG functions associated with the critical exponents. They are reported in App. A 2.

The physically relevant results are obtained by resumming the perturbative expansions (which are divergent but Borel summable), using methods that take into account their large-order behavior, which is computed by semiclassical (hence, intrinsically nonperturbative) instanton calculations [39, 70, 71]. For the model (8) the large-order behavior is discussed in Refs. [61, 68]. The method we use is described in Refs. [39, 71]. Resummations depend on two parameters, which are optimized in the procedure [72].

III. RG PERTURBATIVE RESULTS FOR THE 3D $U(2) \otimes U(2)$ THEORY

In this section we study the 3D RG flow of model (8) in the case relevant for QCD with two light flavors, i.e. for $N = 2$ and $v_0 > 0$. Fig. 1 provides a sketch of the locations of the stable and unstable FPs. The RG trajectories, starting from the unstable Gaussian FP (denoted by G in Fig. 1) of the quadratic theory, flow toward a nontrivial FP (denoted by S) for an extended region of quartic bare parameters v_0 and u_0 , which implies the stability of the FP. We then determine the critical exponents at the stable FP.

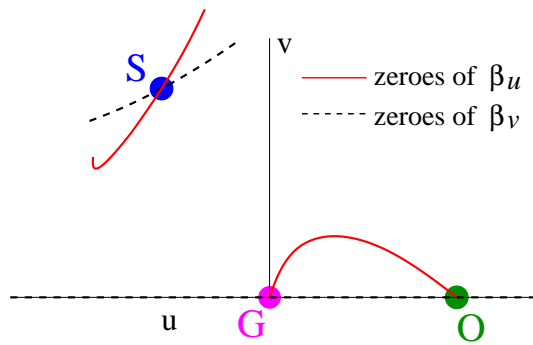


FIG. 1: Zeroes of the β -functions β_u and β_v associated with the quartic couplings of the Lagrangian (8) for $N = 2$. For $v \geq 0$ the β -functions have three common zeroes, corresponding to three FPs: the Gaussian (G) and O(8) (O) FPs along the $v = 0$ axis are unstable, while the FP (S) with $v > 0$ and $u < 0$ is stable.

A. RG trajectories toward the stable FP

We first consider the MZM scheme, where one expands in powers of the zero-momentum renormalized quartic couplings. The theory is renormalized by introducing a set of zero-momentum conditions for the one-particle irreducible two-point and four-point correlation functions of the 2×2 matrix-like field Φ_{ab} :

$$\begin{aligned} \Gamma_{a_1 a_2, b_1 b_2}^{(2)}(p) &= \delta_{a_1 b_1} \delta_{a_2 b_2} Z_\phi^{-1} [m^2 + p^2 + O(p^4)], \quad (9) \\ \Gamma_{a_1 a_2, b_1 b_2, c_1 c_2, d_1 d_2}^{(4)}(0) &= 2\pi Z_\phi^{-2} m^{4-d} \times \\ &\quad \times (u U_{a_1 a_2, b_1 b_2, c_1 c_2, d_1 d_2} + v V_{a_1 a_2, b_1 b_2, c_1 c_2, d_1 d_2}), \quad (10) \end{aligned}$$

where Z_ϕ is the renormalization constant of the order-parameter field Φ , and U, V are appropriate form factors defined so that $u \propto u_0/m$ and $v \propto v_0/m$ at the leading tree order (more details are reported in Ref. [61], where the coupling u, v were denoted by \bar{u}, \bar{v}). The FPs of the theory are given by the common zeroes of the Callan-Symanzik β -functions

$$\beta_u(u, v) = m \frac{\partial u}{\partial m} \Big|_{u_0, v_0}, \quad \beta_v(u, v) = m \frac{\partial v}{\partial m} \Big|_{u_0, v_0}. \quad (11)$$

The resummation of the six-loop series of the β functions, as outlined in Refs. [61, 73], finds a FP (point S in Fig. 1) at [60, 74]

$$u^* = -3.4(3), \quad v^* = 5.3(3), \quad (12)$$

beside the unstable Gaussian FP at $u = v = 0$ and the O(8) FP along the $v = 0$ axis, see Fig. 1. A FP is stable if all eigenvalues of the corresponding stability matrix, $\Omega_{ij} = \partial \beta_i / \partial g_j$ (where $g_{1,2}$ corresponds to u, v) have positive real part. The numerical analysis of the stability matrix at the FP (12) favours its stability [59]. In the following we provide a more direct evidence of the stability of this FP showing that the RG trajectories in the space of the renormalized couplings flow towards this FP for an

extended region of bare parameters. Physically, the values u^* and v^* at a stable FP are the two independent (RG invariant) couplings which describe the zero-momentum behavior of the quartic correlations in the critical region of the disordered phase [7].

The existence of a stable FP is confirmed by the analysis of the β functions in the 3D $\overline{\text{MS}}$ scheme. The renormalized couplings are again defined from the irreducible four-point correlation function, and the $\overline{\text{MS}}$ β functions are

$$\beta_u(u, v) = \mu \frac{\partial u}{\partial \mu} \Big|_{u_0, v_0}, \quad \beta_v(u, v) = \mu \frac{\partial v}{\partial \mu} \Big|_{u_0, v_0}, \quad (13)$$

where μ is the energy scale of this massless scheme. See Ref. [69] for more details. In the 3D $\overline{\text{MS}}$ scheme we set $\epsilon = 4 - d = 1$ and then resum the series using Borel resummation techniques. The five-loop series of the β functions are reported in App. A 2. Again a nontrivial common zero of the β functions is found at [74]

$$u^* = -0.55(6), \quad v^* = 1.22(9), \quad (14)$$

which is represented by the point S in Fig. 1. Note that the renormalized couplings of the MZM and $\overline{\text{MS}}$ perturbative schemes correspond to different quartic couplings, thus their FP values, cf. Eqs. (12) and (14), differ.

In order to check the stability of these FPs and determine their attraction domain, we study the RG flow in the space of the renormalized parameters. If u and v are the renormalized couplings and u_0, v_0 the corresponding Lagrangian couplings that satisfy $u \approx u_0/m$ and $v \approx v_0/m$ at tree level (m is the zero-momentum mass in the MZM scheme and the renormalization energy scale μ in the $\overline{\text{MS}}$ scheme), the RG trajectories are determined by solving the differential equations

$$\begin{aligned} -\lambda \frac{du}{d\lambda} &= \beta_u(u(\lambda), v(\lambda)), \\ -\lambda \frac{dv}{d\lambda} &= \beta_v(u(\lambda), v(\lambda)), \end{aligned} \quad (15)$$

where $\lambda \in [0, \infty)$, with the initial conditions

$$\begin{aligned} u(0) &= v(0) = 0, \\ \frac{du}{d\lambda} \Big|_{\lambda=0} &= s \equiv \frac{u_0}{v_0}, \quad \frac{dv}{d\lambda} \Big|_{\lambda=0} = 1, \end{aligned} \quad (16)$$

where s parametrizes the different RG trajectories in terms of the bare quartic parameters. Note that the initial condition $dv/d\lambda = +1$ for v is required by the theory. Indeed, systems with $v_0 < 0$ are associated with transitions with a different symmetry-breaking pattern, i.e.

$$\text{U}(N_f)_L \otimes \text{U}(N_f)_R \rightarrow \text{U}(N_f - 1)_L \otimes \text{U}(N_f - 1)_R. \quad (17)$$

Since the stability of the Φ^4 theory (8) requires [61]

$$u_0 + v_0 > 0, \quad u_0 + \frac{1}{2}v_0 > 0, \quad (18)$$

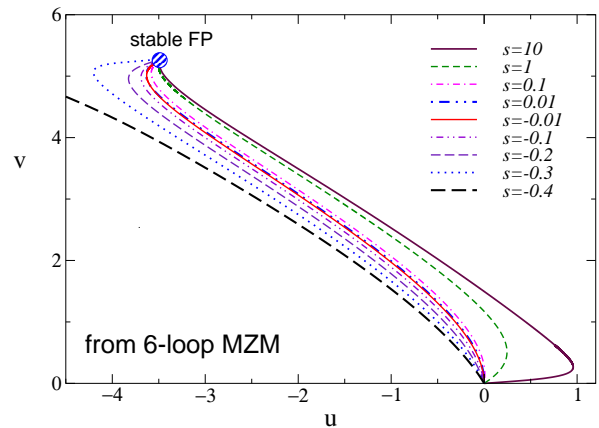


FIG. 2: The RG flow in the renormalized coupling space of the MZM scheme, for several values of the ratio $s \equiv u_0/v_0$ of the bare quartic parameters.

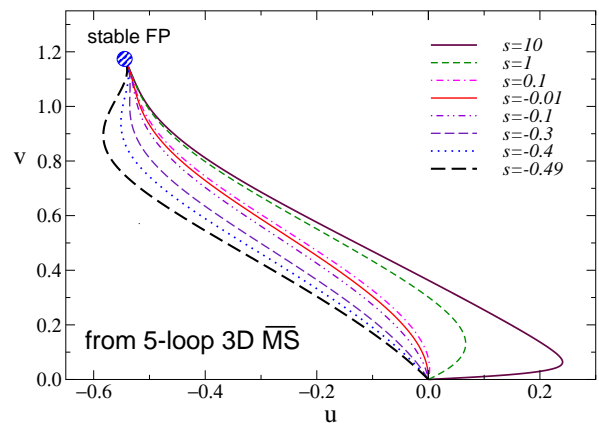


FIG. 3: RG flow in the renormalized coupling space of the massless 3D $\overline{\text{MS}}$ scheme, for several values of the ratio $s \equiv u_0/v_0$ of the bare quartic parameters.

physical systems corresponding to the effective theory (8) with $v_0 > 0$ and $s < -1/2$ are expected to undergo a first-order phase transition.

The RG trajectories for $s > -1/2$ are determined by solving Eq. (15) after resumming the expansions of the β functions. In Figs. 2 and 3 we report the RG flow for several values of the ratio s , as obtained by a particular choice of the approximants that are used to perform the resummation of the perturbative β functions [39, 71, 72]. Different approximants show analogous qualitative behaviors when they are chosen in the optimal region, defined as outlined in Refs. [39, 71]. The RG trajectories in both schemes are attracted by a FP for an extended region of bare quartic parameters u_0, v_0 , which implies that the FP is stable. In the $\overline{\text{MS}}$ scheme, all trajectories with $s \gtrsim -0.5$ flow towards the FP given in Eq. (12), which is indeed the stable FP of the model. In the MZM scheme, we find the same as long as $s \gtrsim -0.4$. The trajectory that corresponds to $s = -0.4$ runs away, into the region in which the perturbative series can no longer be

resummed (the closest Borel singularity is on the positive real axis), hence we are not able to determine its large- λ behavior. In any case, both perturbative schemes show the presence of a stable FP. Moreover, both schemes consistently find that the attraction domain of the bare quartic parameters corresponds to $s = u_0/v_0 \gtrsim -0.5$.

Note that no stable FP is found close to $d = 4$, in agreement with the one-loop ϵ -expansion calculation of Ref. [5], see also Ref. [69]. However, the extension of this result to the relevant $d = 3$ dimension fails. This is not the only physically interesting case in which ϵ -expansion calculations fail to provide the correct physical picture in three dimensions. For example, this also occurs for the Ginzburg-Landau model of superconductors, in which a complex scalar field couples to a gauge field: although ϵ -expansion calculations do not find a stable FP [75], thus predicting first-order transitions, it is now well established (see, e.g., Refs. [76, 77]) that 3D systems described by the Ginzburg-Landau model can also undergo a continuous transition—this implies the presence of a stable FP in the 3D Ginzburg-Landau theory—in agreement with experiments [78]. Other examples are provided by the LGW Φ^4 theories describing frustrated spin models with noncollinear order [68] and the ^3He superfluid transition from the normal to the planar phase [79].

Finally, we also mention that the RG flow of the $U(2)\otimes U(2)$ scalar theory has been also studied by methods based on approximate solutions of functional RG equations. [80, 81] They have not found evidence of a stable FP, but they were limited to approximations keeping only the first terms of the derivative expansion of the effective action.

B. The critical exponents of the $U(2)\otimes U(2)$ Φ^4 theory.

We now compute the critical exponents by evaluating the corresponding RG functions at the stable FP. In the MZM scheme they are given by

$$\eta_\phi(u, v) = \frac{\partial \ln Z_\phi}{\partial \ln m}, \quad \eta_t(u, v) = \frac{\partial \ln Z_t}{\partial \ln m}, \quad (19)$$

where Z_ϕ and Z_t are the renormalization functions of the field Φ and of the quadratic operator $\text{Tr } \Phi^\dagger \Phi$, respectively [61]. The six-loop series are reported in App. A 1. We have performed an analogous calculation in the $\overline{\text{MS}}$ scheme. The perturbative five-loop series are reported in App. A 2.

The critical exponents are obtained by evaluating the resummed RG functions at the stable FP. In particular,

$$\eta = \eta_\phi(u^*, v^*), \quad \nu = [2 - \eta + \eta_t(u^*, v^*)]^{-1}. \quad (20)$$

Resumming the perturbative series by using the conformal-Borel method [39], we obtain

$$\nu = 0.71(7), \quad \eta = 0.12(1), \quad [6 \text{ loop MZM}], \quad (21)$$

$$\nu = 0.76(10), \quad \eta = 0.11(6), \quad [5 \text{ loop } \overline{\text{MS}}]. \quad (22)$$

The errors take into account the uncertainty on the location of the FP, the dependence of the results on the resummation parameters and the stability of the estimates with respect to the number of terms in the series [74].

Estimates (21) and (22) obtained in the two perturbative schemes are fully consistent. This agreement provides a nontrivial crosscheck of the accuracy of the analysis of the MZM and 3D $\overline{\text{MS}}$ perturbative series: the resummation of the perturbative expansions in two different schemes give consistent results for the universal quantities. This fact may be hardly explained as an artefact of the resummation; it should instead be considered as a robust evidence of the existence of a stable FP describing 3D continuous transitions characterized by the symmetry-breaking pattern $U(2)\otimes U(2)\rightarrow U(2)$.

IV. CONCLUSIONS

In this paper we report a detailed study of the RG flow of the Φ^4 model (8) for $N = 2$, which is relevant for the finite- T chiral transition of two-flavor QCD if the $U(1)_A$ symmetry is restored at the chiral transition. For this purpose we consider two field-theoretical perturbative schemes: the MZM scheme, defined in the disordered massive phase, and the 3D $\overline{\text{MS}}$ scheme without ϵ expansion, which considers the massless critical theory. Extending previous RG studies [59–61], we verify the existence of a stable FP with $v_0 > 0$, which is the relevant domain for the symmetry-breaking pattern (6). We study the RG flow in the space of the renormalized quartic couplings, as obtained by the analysis of the perturbative expansions of the β functions, computed to six and five loops in the MZM and 3D $\overline{\text{MS}}$ scheme, respectively. In both cases the RG trajectories starting from the unstable Gaussian FP flow towards a nontrivial stable FP for an extended region of the bare quartic parameters u_0, v_0 , i.e. for $u_0/v_0 \gtrsim -0.5$. This implies that systems corresponding to an effective Lagrangian with $u_0/v_0 \gtrsim -0.5$ undergo a continuous transition. We also estimate the corresponding critical exponents, obtaining consistent results in the two field-theoretical schemes considered, cf. Eqs. (21) and (22). On the other hand, systems corresponding to $u_0/v_0 \lesssim -0.5$ are expected to undergo a first-order transition.

The existence of a stable FP with $v > 0$ implies that the finite- T chiral transition of two-flavor QCD can be continuous also if the $U(1)_A$ symmetry is effectively restored at T_c . Although the critical behavior differs from that expected in the case of a substantial $U(1)_A$ symmetry breaking around T_c , which is the 3D $O(4)$ vector universality class, we note that differences are small. For instance, the critical exponents of the $O(4)$ universality class [9, 13], $\nu = 0.749(2)$, $\eta = 0.0365(10)$, $\delta = (5 - \eta)/(1 + \eta) \approx 4.789(6)$, $\beta = \nu(1 + \eta)/2 \approx 0.388(1)$, $\gamma = \nu(2 - \eta) = 1.471(4)$ and $\alpha = 2 - 3\nu = -0.247(6)$ are close to those we have obtained for model (8). In the MZM scheme we obtain $\nu = 0.71(7)$, $\eta = 0.12(1)$,

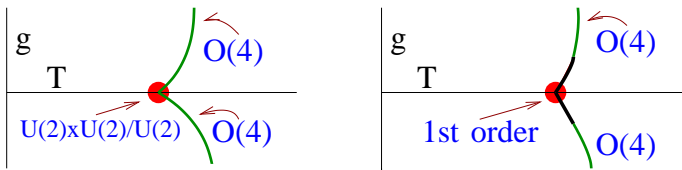


FIG. 4: Possible phase diagrams in the T - g plane for the effective model with symmetry-breaking pattern (4). The parameter g is proportional to the $U(1)_A$ symmetry breaking, hence for $g = 0$ we reobtain the model with symmetry-breaking pattern (6). On the left panel, the multicritical transition at $g = 0$ is continuous, on the right panel it is of first order. Thick black lines indicate first-order transitions. The endpoints of the first-order transition lines correspond to mean-field transitions with logarithmic corrections.

$\delta = 4.3(1)$, $\beta = 0.40(4)$, $\gamma = 1.3(1)$, and $\alpha = 0.1(2)$. In the $\overline{\text{MS}}$ scheme we obtain instead $\nu = 0.76(10)$, $\eta = 0.11(6)$, $\delta = 4.4(3)$, $\beta = 0.42(6)$, $\gamma = 1.4(2)$, and $\alpha = -0.3(3)$. Thus, only very accurate estimates of the critical exponents can distinguish the two different critical behaviors.

We stress that the existence of a universality class does not exclude that some systems with the same order parameter and symmetry-breaking pattern undergo a first-order transition. This occurs when the system is outside the attraction domain of the stable FP, i.e., when the system at the transition is effectively described by the Lagrangian (8) with quartic parameters u_0 and v_0 belonging to the large region $u_0/v_0 \lesssim -0.5$. The nature (first-order or continuous) of the transition is nonuniversal, since it depends on the details of the model and not only on the global features that characterize the universality class. For example, the model considered in Ref. [82], which corresponds to two-flavor lattice QED with the same symmetry breaking $U(2)_L \otimes U(2)_R \rightarrow U(2)_V$, shows a first-order transition. This result cannot be extended to all transitions with the same symmetry breaking, because it is indeed possible that this model corresponds to a runaway RG trajectory, while the case relevant to QCD may belong to the attraction domain of the stable FP, thus undergoing a continuous transition.

The results for model (8) are also of interest if chiral symmetry is not exactly restored at T_c , but $U(1)_A$ breaking effects are small. In this case we can parametrize the effective Lagrangian as

$$\mathcal{L}_{\text{SU}(2)} = \mathcal{L}_{\text{U}(2)} + w_0 (\det\Phi^\dagger + \det\Phi) + \frac{x_0}{4} (\text{Tr}\Phi^\dagger\Phi) (\det\Phi^\dagger + \det\Phi) + \frac{y_0}{4} [(\det\Phi^\dagger)^2 + (\det\Phi)^2], \quad (23)$$

where we added all terms up to dimension four which contain the determinant of the 2×2 order parameter field and leave a residual $SU(2) \otimes SU(2)$ symmetry. In the context of two-flavor QCD, we may assume that $w_0, x_0, y_0 \sim g$ where g parametrizes the effective breaking of the $U(1)_A$ symmetry. In the T - g plane, the $U(2)_L \otimes U(2)_R$ transition point becomes a multicritical point [61], as Lagrangian

(23) contains two quadratic terms. In Fig. 4 we show two possible phase diagrams, depending on the nature of the transition at $g = 0$. In the first case (left panel of Fig. 4), the transition is always continuous for $g \neq 0$ along the critical line $T_c(g)$. But if $|g|$ is small, we may observe a crossover behavior controlled by the $U(2) \otimes U(2)$ multicritical point at $g = 0$: the free energy should behave as $\mathcal{F}_{\text{sing}} \approx t^{3\nu} f(gt^{-\phi})$, where $t \propto T - T_c(g = 0)$, $\nu \approx 0.7$, and $\phi \approx 1.3$ [83]. In practice, if g is small, one might observe two different behaviors depending on the distance of T from the critical line $T_c(g)$. For $|T - T_c(g)|$ not too small, the RG flow is influenced by the $U(2) \otimes U(2)$ multicritical point, hence one would observe an effective critical behavior analogous to that for $g = 0$. As T approaches $T_c(g)$, this crossover behavior disappears and the $O(4)$ behavior is eventually observed. In the other case, shown in the right panel of Fig. 4, we expect first-order transitions to occur also for $|g|$ small, up to an endpoint g^* where mean-field behavior with logarithmic corrections should be observed; then the continuous transition for larger $g > g^*$ (note that g^* does not need to be small) is expected to belong to the $O(4)$ universality class. The available numerical MC results for QCD with two light flavors do not yet allow us to distinguish between the above scenarios.

Finally, we would like to discuss the possible scenarios for the finite- T transitions of the QCD-like theory with a large number N_c of colors, widening the parameter space to get further hints for the relevant $N_c = 3$ case. We first note that the universality arguments based on the global flavor symmetries do not depend on the number of colors, thus they hold for any $N_c > 3$ (keeping N_f fixed) as well, including $N_c \rightarrow \infty$. At large N_c , keeping the number N_f of flavors fixed, we expect a first-order transition corresponding to the deconfinement transition of pure $SU(N_c)$ gauge theories for a large number of colors, thus at [84, 85] $T_c/\sqrt{\sigma} = 0.545(2) + O(N_c^{-2})$ where σ is the string tension. The presence of $N_f = 2$ fermion flavors, which contribute to $O(1/N_c)$ according to standard large- N_c scaling arguments [86], cannot smooth out this transition whose latent heat is $O(N_c^2)$ [87–89]. This opens the road to other possible scenarios with respect to the standard three-color QCD. Indeed, the chiral symmetry of the fermions may be restored at the same transition point, or we may have another transition at a larger temperature [89], like the case of QCD with adjoint fermions [90, 91], where the deconfinement and chiral transitions occur at different temperatures. Moreover, since the $U(1)_A$ anomaly is suppressed by $1/N_c$ in the large- N_c limit [92], the $U(1)_A$ symmetry breaking is further suppressed at large N_c , as also shown by the behavior $\chi_\pi - \chi_\delta \sim T^{-\kappa}$, where the exponent $\kappa \sim N_c$, cf. Eq. (5). Therefore, with increasing N_c , the effective symmetry breaking at the chiral transition with two light flavors should be better and better described by $U(2)_L \otimes U(2)_R \rightarrow U(2)_V$, rather than $SU(2)_L \otimes SU(2)_R \rightarrow SU(2)_V$.

Acknowledgements. We thank Claudio Bonati and

Massimo D'Elia for useful discussions.

Φ^4 theory (8) and estimate the critical exponents, i.e. the six-loop series of the MZM scheme and the five-loop series of the 3D $\overline{\text{MS}}$ scheme.

Appendix A: High-order perturbative series of the $U(2) \otimes U(2)$ Φ^4 theory

In this appendix we report the perturbative series used in the paper to analyze the RG flow of the $U(2) \otimes U(2)$

1. The MZM series up to six loops

The β functions of the MZM perturbative schemes have been already reported to six loops in Ref. [61]. Here we report the six-loop RG functions defined in Eq. (19), which allow us to evaluate the critical exponents through Eqs. (20). They are given by

$$\begin{aligned} \eta_\phi(u, v) = & 0.011574074u^2 + 0.000964218u^3 + 0.001280763u^4 - 0.000212863u^5 + 0.000487251u^6 \\ & + 0.018518518uv + 0.002314125u^2v + 0.004098443u^3v - 0.00085145u^4v + 0.00233880u^5v \\ & + 0.011574074v^2 + 0.002241809uv^2 + 0.00595656u^2v^2 - 0.00169549u^3v^2 + 0.00540470u^4v^2 \\ & + 0.000771375v^3 + 0.00417400uv^3 - 0.00183407u^2v^3 + 0.0071929u^3v^3 \\ & + 0.00105250v^4 + 0.000956991uv^4 + 0.00550762u^2v^4 - 0.000180727v^5 + 0.00223754uv^5 + 0.000372148v^6, \end{aligned} \quad (\text{A1})$$

and

$$\begin{aligned} \eta_t(u, v) = & -0.625u + 0.078125u^2 - 0.053818796u^3 + 0.0282218u^4 - 0.0265992u^5 + 0.0230998u^6 \\ & - 0.5v + 0.125uv - 0.12916511u^2v + 0.0903098u^3v - 0.10639677u^4v + 0.11087907u^5v \\ & + 0.078125v^2 - 0.12444547uv^2 + 0.13414445u^2v^2 - 0.19715907u^3v^2 + 0.2561752u^4v^2 \\ & - 0.0430550v^3 + 0.0964956uv^3 - 0.1970603u^2v^3 + 0.3409476u^3v^3 \\ & + 0.0241934v^4 - 0.0993356uv^4 + 0.260895u^2v^4 - 0.0193974v^5 + 0.1057591uv^5 + 0.017517v^6. \end{aligned} \quad (\text{A2})$$

2. The $\overline{\text{MS}}$ series up to five loops

We report the perturbative series in the $\overline{\text{MS}}$ scheme. The β functions were computed in Ref. [69], where they were explicitly reported up to three loops for generic $U(M) \otimes U(N)$ models. Here we report the five-loop series of the β functions and of the RG functions associated with the critical exponents for the case relevant for QCD with two flavors, i.e. the Φ^4 theory (8) with $N = 2$.

The β functions are given by [93]

$$\begin{aligned} \beta_u(u, v) = & -u + 4u^2 + 4uv + \frac{3}{2}v^2 - \frac{57}{8}u^3 - 11u^2v - \frac{61}{8}uv^2 - 3v^3 + \frac{93}{8}u^4\zeta(3) + \frac{389}{16}u^4 + 24u^3v\zeta(3) + \frac{975}{16}u^3v \\ & + \frac{99}{4}u^2v^2\zeta(3) + \frac{9347}{128}u^2v^2 + 18uv^3\zeta(3) + 45uv^3 + 6v^4\zeta(3) + \frac{1197}{128}v^4 - \frac{1885}{16}u^5\zeta(5) - \frac{3119}{32}u^5\zeta(3) + \frac{31}{120}\pi^4u^5 \\ & - \frac{51759}{512}u^5 - 340u^4v\zeta(5) - \frac{1183}{4}u^4v\zeta(3) + \frac{161}{240}\pi^4u^4v - \frac{10449u^4}{32}v - \frac{3905}{8}u^3v^2\zeta(5) - \frac{6849}{16}u^3v^2\zeta(3) + \frac{353}{480}\pi^4u^3v^2 \\ & - \frac{391151}{768}u^3v^2 - \frac{895}{2}u^2v^3\zeta(5) - 377u^2v^3\zeta(3) + \frac{8}{15}\pi^4u^2v^3 - \frac{42919}{96}u^2v^3 - \frac{1875}{8}uv^4\zeta(5) - \frac{3049}{16}uv^4\zeta(3) \\ & + \frac{31}{96}\pi^4uv^4 - \frac{12697}{64}uv^4 - 50v^5\zeta(5) - \frac{325}{8}v^5\zeta(3) + \frac{5}{48}\pi^4v^5 - \frac{1097}{32}v^5 + \frac{646947}{512}u^6\zeta(7) + \frac{333739}{256}u^6\zeta(5) \\ & - \frac{3}{64}u^6\zeta(3)^2 + \frac{333239}{512}u^6\zeta(3) - \frac{1885}{4032}\pi^6u^6 - \frac{6827}{2560}\pi^4u^6 + \frac{121665}{256}u^6 + \frac{146853}{32}u^5v\zeta(7) + \frac{158151}{32}u^5v\zeta(5) \\ & - \frac{507}{32}u^5v\zeta(3)^2 + \frac{320791}{128}u^5v\zeta(3) - \frac{6625}{4032}\pi^6u^5v - \frac{37481}{3840}\pi^4u^5v + \frac{494921}{256}u^5v + \frac{4266675}{512}u^4v^2\zeta(7) + \frac{1144635}{128}u^4v^2\zeta(5) \\ & - \frac{7017}{256}u^4v^2\zeta(3)^2 + \frac{4795927}{1024}u^4v^2\zeta(3) - \frac{9615}{3584}\pi^6u^4v^2 - \frac{504343}{30720}\pi^4u^4v^2 + \frac{7852881}{2048}u^4v^2 + 9702u^3v^3\zeta(7) + \frac{79415}{8}u^3v^3\zeta(5) \\ & - \frac{3}{4}u^3v^3\zeta(3)^2 + \frac{171801}{32}u^3v^3\zeta(3) - \frac{155}{56}\pi^6u^3v^3 - \frac{8173}{480}\pi^4u^3v^3 + \frac{6814435}{1536}u^3v^3 + \frac{3658095}{512}u^2v^4\zeta(7) + \frac{1773961}{256}u^2v^4\zeta(5) \\ & + \frac{2777}{128}u^2v^4\zeta(3)^2 + \frac{1942077}{512}u^2v^4\zeta(3) - \frac{94645}{48384}\pi^6u^2v^4 - \frac{182363}{15360}\pi^4u^2v^4 + \frac{36147287}{12288}u^2v^4 + \frac{189189}{64}uv^5\zeta(7) \\ & + \frac{44351}{16}uv^5\zeta(5) + \frac{103}{8}uv^5\zeta(3)^2 + \frac{189841}{128}uv^5\zeta(3) - \frac{2585}{3024}\pi^6uv^5 - \frac{1647}{320}\pi^4uv^5 + \frac{2121643}{2048}uv^5 \\ & + \frac{265041}{512}v^6\zeta(7) + \frac{61459}{128}v^6\zeta(5) + \frac{81}{64}v^6\zeta(3)^2 + \frac{246291}{1024}v^6\zeta(3) - \frac{335}{2016}\pi^6v^6 - \frac{3125}{3072}\pi^4v^6 + \frac{2538035}{16384}v^6, \end{aligned} \quad (\text{A3})$$

$$\begin{aligned}
\beta_v(u, v) = & -v + 3uv + 2v^2 - \frac{61}{8}u^2v - 11uv^2 - \frac{27}{8}v^3 + \frac{1349}{64}u^3v + \frac{1451}{32}u^2v^2 + \frac{575}{16}uv^3 + \frac{347}{32}v^4 + \frac{33}{2}u^3v\zeta(3) \\
& + 36u^2v^2\zeta(3) + 24uv^3\zeta(3) + \frac{9}{2}v^4\zeta(3) - \frac{49815}{512}u^4v + \frac{29}{64}\pi^4u^4v - \frac{27835}{96}u^3v^2 + \frac{163}{120}\pi^4u^3v^2 - \frac{279945}{768}u^2v^3 + \frac{22}{15}\pi^4u^2v^3 \\
& - \frac{6635}{32}uv^4 + \frac{53}{80}\pi^4uv^4 - \frac{365}{8}v^5 + \frac{1}{10}\pi^4v^5 - \frac{3765}{32}u^4v\zeta(3) - \frac{691}{2}u^3v^2\zeta(3) - \frac{6111}{16}u^2v^3\zeta(3) - \frac{1507}{8}uv^4\zeta(3) - \frac{567}{16}v^5\zeta(3) \\
& - \frac{2625}{16}u^4v\zeta(5) - 480u^3v^2\zeta(5) - \frac{2115}{4}u^2v^3\zeta(5) - \frac{1045}{4}uv^4\zeta(5) - \frac{795}{16}v^5\zeta(5) + \frac{445355}{1024}u^5v - \frac{58367}{15360}\pi^4u^5v \\
& - \frac{12115}{16128}\pi^6u^5v + \frac{209163}{128}u^4v^2 - \frac{109087}{7680}\pi^4u^4v^2 - \frac{7535}{2688}\pi^6u^4v^2 + \frac{16837765}{6144}u^3v^3 - \frac{81491}{3840}\pi^4u^3v^3 - \frac{8455}{2016}\pi^6u^3v^3 \\
& + \frac{3808447}{1536}u^2v^4 - \frac{30289}{1920}\pi^4u^2v^4 - \frac{38005}{12096}\pi^6u^2v^4 + \frac{9331663}{8192}uv^5 - \frac{1485}{256}\pi^4uv^5 - \frac{28555}{24192}\pi^6uv^5 + \frac{825245}{4096}v^6 - \frac{1285}{1536}\pi^4v^6 \\
& - \frac{5}{28}\pi^6v^6 + \frac{395479}{512}u^5v\zeta(3) + \frac{734983}{256}u^4v^2\zeta(3) + \frac{282653}{64}u^3v^3\zeta(3) + \frac{56043}{16}u^2v^4\zeta(3) + \frac{736561}{512}uv^5\zeta(3) + \frac{63485}{256}v^6\zeta(3) \\
& + \frac{2499}{128}u^5v\zeta(3)^2 + \frac{4305}{64}u^4v^2\zeta(3)^2 + \frac{405}{4}u^3v^3\zeta(3)^2 + \frac{2771}{32}u^2v^4\zeta(3)^2 + \frac{2579}{64}uv^5\zeta(3)^2 + \frac{231}{32}v^6\zeta(3)^2 + \frac{105231}{64}u^5v\zeta(5) \\
& + \frac{390003}{64}u^4v^2\zeta(5) + \frac{295491}{32}u^3v^3\zeta(5) + \frac{457495}{64}u^2v^4\zeta(5) + \frac{5647}{2}uv^5\zeta(5) + \frac{29035}{64}v^6\zeta(5) + \frac{472311}{256}u^5v\zeta(7) \\
& + \frac{218295}{32}u^4v^2\zeta(7) + \frac{1325205}{128}u^3v^3\zeta(7) + \frac{1030617}{128}u^2v^4\zeta(7) + \frac{816291}{256}uv^5\zeta(7) + \frac{16317}{32}v^6\zeta(7). \tag{A4}
\end{aligned}$$

The five-loop series of the RG functions associated with the critical exponents are

$$\begin{aligned}
\eta_\phi(u, v) = & + \frac{5}{16}u^2 + \frac{1}{2}uv + \frac{5}{16}v^2 - \frac{5}{16}u^3 - \frac{3}{4}u^2v - \frac{93}{128}uv^2 - \frac{1}{4}v^3 \\
& + \frac{1125}{1024}u^4 + \frac{225}{64}u^3v + \frac{2835}{512}u^2v^2 + \frac{135}{32}uv^3 + \frac{135}{128}v^4 - \frac{485}{64}u^5 - \frac{31}{1536}\pi^4u^5 - \frac{485}{16}u^4v - \frac{31}{384}\pi^4u^4v \\
& - \frac{114469}{2048}u^3v^2 - \frac{119}{768}\pi^4u^3v^2 - \frac{28337}{512}u^2v^3 - \frac{31}{192}\pi^4u^2v^3 - \frac{57059}{2048}uv^4 - \frac{1}{12}\pi^4uv^4 - \frac{5743}{1024}v^5 - \frac{31}{1920}\pi^4v^5 + \frac{515}{512}u^5\zeta(3) \\
& + \frac{515}{128}u^4v\zeta(3) + \frac{3593}{512}u^3v^2\zeta(3) + \frac{407}{64}u^2v^3\zeta(3) + \frac{1513}{512}uv^4\zeta(3) + \frac{19}{32}v^5\zeta(3), \tag{A5}
\end{aligned}$$

$$\begin{aligned}
\eta_t(u, v) = & -\frac{5u}{2} - 2v + \frac{15}{8}u^2 + 3uv + \frac{15}{8}v^2 - \frac{1195}{128}u^3 - \frac{717}{32}u^2v - \frac{2775}{128}uv^2 - \frac{239}{32}v^3 + \frac{9825}{256}u^4 + \frac{31}{384}\pi^4u^4 + \frac{1965}{16}u^3v \\
& + \frac{31}{120}\pi^4u^3v + \frac{1431}{8}u^2v^2 + \frac{119}{320}\pi^4u^2v^2 + \frac{4029}{32}uv^3 + \frac{31}{120}\pi^4uv^3 + \frac{8103}{256}v^4 + \frac{1}{15}\pi^4v^4 + \frac{425}{64}u^4\zeta(3) + \frac{85}{4}u^3v\zeta(3) \\
& + \frac{51}{2}u^2v^2\zeta(3) + \frac{107}{8}uv^3\zeta(3) + \frac{209}{64}v^4\zeta(3) - \frac{398085}{2048}u^5 - \frac{2503}{6144}\pi^4u^5 - \frac{9425}{96768}\pi^6u^5 - \frac{398085}{512}u^4v - \frac{2503}{1536}\pi^4u^4v \\
& - \frac{9425}{24192}\pi^6u^4v - \frac{5888529}{4096}u^3v^2 - \frac{24209}{7680}\pi^4u^3v^2 - \frac{34885}{48384}\pi^6u^3v^2 - \frac{366513}{256}u^2v^3 - \frac{12767}{3840}\pi^4u^2v^3 - \frac{8705}{12096}\pi^6u^2v^3 \\
& - \frac{11832549}{16384}uv^4 - \frac{26999}{15360}\pi^4uv^4 - \frac{17735}{48384}\pi^6uv^4 - \frac{589857}{4096}v^5 - \frac{691}{1920}\pi^4v^5 - \frac{1795}{24192}\pi^6v^5 - \frac{102955}{1024}u^5\zeta(3) - \frac{102955}{256}u^4v\zeta(3) \\
& - \frac{364439}{512}u^3v^2\zeta(3) - \frac{85837}{128}u^2v^3\zeta(3) - \frac{334685}{1024}uv^4\zeta(3) - \frac{16379}{256}v^5\zeta(3) + \frac{4675}{256}u^5\zeta(3)^2 + \frac{4675}{64}u^4v\zeta(3)^2 + \frac{17687}{128}u^3v^2\zeta(3)^2 \\
& + \frac{4531}{32}u^2v^3\zeta(3)^2 + \frac{9307}{128}uv^4\zeta(3)^2 + \frac{917}{64}v^5\zeta(3)^2 + \frac{85}{64}u^5\zeta(5) + \frac{85}{16}u^4v\zeta(5) + \frac{1601}{128}u^3v^2\zeta(5) + \frac{65}{4}u^2v^3\zeta(5) \\
& + \frac{461}{64}uv^4\zeta(5) - \frac{1}{16}v^5\zeta(5). \tag{A6}
\end{aligned}$$

-
- | | |
|--|---|
| <p>[1] F. Wilczek, <i>Int. J. Mod. Phys. A</i> 07, 3911 (1992).
 [2] K. Rajagopal and F. Wilczek, <i>Nucl. Phys. B</i> 399, 395 (1993).
 [3] F. Wilczek, arXiv:hep-ph/0003183.
 [4] F. Karsch, <i>Lect. Notes Phys.</i> 583, 209 (2002).
 [5] R. D. Pisarski and F. Wilczek, <i>Phys. Rev. D</i> 29, 338 (1984).
 [6] S. Gavin, A. Gocksch, and R. D. Pisarski, <i>Phys. Rev. D</i> 49, R3079 (1994).
 [7] A. Pelissetto and E. Vicari, <i>Phys. Rep.</i> 368, 549 (2002).
 [8] R. Guida and J. Zinn-Justin, <i>J. Phys. A</i> 31, 8103 (1998).
 [9] M. Hasenbusch, <i>J. Phys. A</i> 34, 8221 (2001).
 [10] F. Parisen Toldin, A. Pelissetto, and E. Vicari, <i>J. High Energy Phys.</i> 07, 029 (2003).
 [11] J. Engels, L. Fromme, and M. Seniuch, <i>Nucl. Phys. B</i> 675, 533 (2003).
 [12] Y. Deng, <i>Phys. Rev. E</i> 73, 056116 (2006).
 [13] M. Hasenbusch and E. Vicari, <i>Phys. Rev. B</i> 84, 125136 (2011).</p> | <p>[14] J. Engels and F. Karsch, <i>Phys. Rev. D</i> 85, 094506 (2012).
 [15] J. Berges, D.-U. Jungnickel, and C. Wetterich, <i>Phys. Rev. D</i> 59, 034010 (1999).
 [16] D. J. Gross, R. D. Pisarski, and L. G. Yaffe, <i>Rev. Mod. Phys.</i> 53, 43 (1981).
 [17] A. Bazavov, T. Bhattacharya, M. I. Buchoff, M. Cheng, N. H. Christ, H.-T. Ding, R. Gupta, P. Hegde, C. Jung, F. Karsch, Z. Lin, R. D. Mawhinney, S. Mukherjee, P. Petreczky, R. A. Soltz, P. M. Vranas, and H. Yin, <i>Phys. Rev. D</i> 86, 094503 (2012).
 [18] S. Chandrasekharan, D. Chen, N. H. Christ, W.-J. Lee, R. D. Mawhinney, and P. Vranas, <i>Phys. Rev. Lett.</i> 82, 2463 (1999).
 [19] M. I. Buchoff, M. Cheng, N. H. Christ, H.-T. Ding, C. Jung, F. Karsch, R. D. Mawhinney, S. Mukherjee, P. Petreczky, D. Renfrew, C. Schroeder, P. M. Vranas, H. Yin, and Z. Lin, arXiv:1309.4149.
 [20] G. Cossu, S. Aoki, H. Fukaya, S. Hashimoto, T. Kaneko, H. Matsufuru, and J.-I. Noaki, <i>Phys. Rev. D</i> 87, 114514</p> |
|--|---|

- (2013).
- [21] S. Aoki, H. Fukaya, and Y. Taniguchi, Phys. Rev. D **86**, 114512 (2012).
- [22] F. Karsch, Nucl. Phys. (Proc. Suppl.) **83**, 14 (2000).
- [23] P. M. Vranas, Nucl. Phys. (Proc. Suppl.) **83**, 414 (2000).
- [24] J. B. Kogut, J.-F. Lagaë, and D. K. Sinclair, Phys. Rev. D **58**, 054504 (1998).
- [25] C. Bernard, T. Blum, C. De Tar, S. Gottlieb, U. M. Heller, J.E. Hetrick, K. Rummukainen, R. Sugar, D. Toussaint, and M. Wingate, Phys. Rev. Lett. **78**, 598 (1997).
- [26] M. Grahl and D. H. Rischke, Phys. Rev. D **88**, 056014 (2013).
- [27] M. Mitter and B. Schaefer, arXiv:1308.3176.
- [28] E. Meggiolaro and A. Mordá, arXiv:1309.4598.
- [29] J. M. Pawłowski, Phys. Rev. D **58**, 045011 (1998).
- [30] M. C. Birse, T. D. Cohen, and J. A. McGovern, Phys. Lett. B **388**, 137 (1996); Phys. Lett. B **399**, 263 (1997).
- [31] N. Evans, D. D. Hsu, and M. Schwetz, Phys. Lett. B **375**, 262 (1996).
- [32] S. H. Lee and T. Hatsuda, Phys. Rev. D **54**, R1871 (1996).
- [33] T. D. Cohen, Phys. Rev. D **54**, R1867 (1996).
- [34] E. V. Shuryak, Comments Nucl. Part. Phys. **21**, 235 (1994).
- [35] E. Vicari and H. Panagopoulos, Phys. Rep. **470**, 93 (2009).
- [36] C. Bonati, M. D'Elia, H. Panagopoulos, and E. Vicari, Phys. Rev. Lett. **110**, 252003 (2013).
- [37] K. G. Wilson and J. Kogut, Phys. Rep. **12**, 75 (1974).
- [38] M. E. Fisher, Rev. Mod. Phys. **46**, 597 (1974).
- [39] J. Zinn-Justin, *Quantum Field Theory and Critical Phenomena*, fourth edition (Clarendon Press, Oxford, 2002).
- [40] A. Ali Khan, S. Aoki, R. Burkhalter, S. Ejiri, M. Fukugita, S. Hashimoto, N. Ishizuka, Y. Iwasaki, K. Kanaya, T. Kaneko, Y. Kuramashi, T. Manke, K. Nagai, M. Okamoto, M. Okawa, A. Ukawa, and T. Yoshié (CP-PACS Collaboration), Phys. Rev. D **63**, 034502 (2000).
- [41] C. Bernard, T. Burch, T. A. DeGrand, C. E. De Tar, S. Gottlieb, U. M. Heller, J.E. Hetrick, K. Orginos, R. L. Sugar, and D. Toussaint (MILC Collaboration), Phys. Rev. D **61**, 111502 (2000).
- [42] F. Karsch, E. Laermann, and A. Peikert, Nucl. Phys. B **605**, 579 (2001).
- [43] J. B. Kogut and D. K. Sinclair, Phys. Rev. D **64**, 034508 (2001).
- [44] J. Engels, S. Holtmann, T. Mendes, and T. Schulze, Phys. Lett. B **514**, 299 (2001).
- [45] M. D'Elia, A. Di Giacomo, and C. Pica, Phys. Rev. D **72**, 114510 (2005); G. Cossu, M. D'Elia, A. Di Giacomo, and C. Pica, arXiv:0706.4470.
- [46] J. B. Kogut and D. K. Sinclair, Phys. Rev. D **73**, 074512 (2006).
- [47] P. de Forcrand and O. Philipsen, J. High Energy Phys. **01**, 077 (2007).
- [48] C. Bonati, P. de Forcrand, M. D'Elia, O. Philipsen, and F. Sanfilippo, Proc. Sci. LATTICE2011 (2011) 189.
- [49] A. Bazavov, T. Bhattacharya, M. Cheng, C. DeTar, H.-T. Ding, Steven Gottlieb, R. Gupta, P. Hegde, U. M. Heller, F. Karsch, E. Laermann, L. Levkova, S. Mukherjee, P. Petreczky, C. Schmidt, R. A. Soltz, W. Soeldner, R. Sugar, D. Toussaint, W. Unger, and P. Vranas, Phys. Rev. D **85**, 054503 (2012).
- [50] F. Burger, E.-M. Ilgenfritz, M. Kirchner, M. P. Lombardo, M. Müller-Preussker, O. Philipsen, C. Pinke, C. Urbach, and L. Zeidlewicz, Phys. Rev. D **87**, 074508 (2013).
- [51] C. Bernard, T. Burch, C. DeTar, J. Osborn, S. Gottlieb, E. B. Gregory, U. M. Heller, J. Osborn, R. Sugar, and D. Toussaint (MILC collaboration), Phys. Rev. D **71**, 034504 (2005).
- [52] Y. Aoki, Z. Fodor, S. D. Katz, and K. K. Szabo, Phys. Lett. B **643**, 46 (2006).
- [53] M. Cheng, N. H. Christ, S. Datta, J. van der Heide, C. Jung, F. Karsch, O. Kaczmarek, E. Laermann, R. D. Mawhinney, C. Miao, P. Petreczky, K. Petrov, C. Schmidt, and T. Umeda, Phys. Rev. D **74**, 054507 (2006).
- [54] Y. Aoki, G. Endrodi, Z. Fodor, S. D. Katz, and K. K. Szabo, Nature **443**, 675 (2006).
- [55] A. Bazavov, T. Bhattacharya, M. Cheng, N. H. Christ, C. DeTar, S. Ejiri, S. Gottlieb, R. Gupta, U. M. Heller, K. Huebner, C. Jung, F. Karsch, E. Laermann, L. Levkova, C. Miao, R. D. Mawhinney, P. Petreczky, C. Schmidt, R. A. Soltz, W. Soeldner, R. Sugar, D. Toussaint, and P. Vranas, Phys. Rev. D **80**, 014504 (2009).
- [56] Y. Aoki, Sz. Borsanyi, S. Durr, Z. Fodor, S. D. Katz, S. Krieg, and K. K. Szabo, J. High Energy Phys. **06**, 088 (2009).
- [57] M. Cheng, S. Ejiri, P. Hegde, F. Karsch, O. Kaczmarek, E. Laermann, R.D. Mawhinney, C. Miao, S. Mukherjee, P. Petreczky, C. Schmidt, and W. Soeldner, Phys. Rev. D **81**, 054504 (2010).
- [58] S. Borsanyi, Z. Fodor, C. Hoelbling, S. D. Katz, S. Krieg, C. Ratti, and K. K. Szabo (Wuppertal-Budapest Collaboration), J. High Energy Phys. **09**, 073 (2010).
- [59] F. Basile, A. Pelissetto, and E. Vicari, PoS (LAT2005) 199 (2005).
- [60] F. Basile, A. Pelissetto, and E. Vicari, J. High Energy Phys. **02**, 044 (2005).
- [61] A. Butti, A. Pelissetto, and E. Vicari, J. High Energy Phys. **08**, 029 (2003).
- [62] G. Parisi, Cargèse Lectures (1973); J. Stat. Phys. **23**, 49 (1980).
- [63] V. Dohm, Z. Phys. B **60**, 61 (1985); Z. Phys. B **61**, 193 (1985).
- [64] R. Schloms and V. Dohm, Nucl. Phys. B **328**, 639 (1989).
- [65] E. Vicari, PoS (LAT2007) 023 (2007).
- [66] G. 't Hooft and M. J. G. Veltman, Nucl. Phys. B **44**, 189 (1972).
- [67] K. G. Wilson and M. E. Fisher, Phys. Rev. Lett. **28**, 240 (1972).
- [68] P. Calabrese, P. Parruccini, A. Pelissetto, and E. Vicari, Phys. Rev. B **70**, 174439 (2004).
- [69] P. Calabrese and P. Parruccini, J. High Energy Phys. **05**, 018 (2004).
- [70] J. C. Le Guillou and J. Zinn-Justin, Phys. Rev. Lett. **39**, 95 (1977); Phys. Rev. B **21**, 3976 (1980).
- [71] J.M. Carmona, A. Pelissetto, and E. Vicari, Phys. Rev. B **61**, 15136 (2000).
- [72] The approximants we use depend on two parameters α and b ; we use here the notations of Refs. [39, 71]. In particular, the RG trajectories reported in Figs. 2 and 3 are obtained by using $\alpha = 2$ and $b = 5$ for β_u and $\alpha = 1$ and $b = 5$ for β_v in both schemes.
- [73] The first analysis of the MZM β functions, reported in Ref. [61], was performed in the domain $-2 \lesssim u \lesssim 4$, $0 < v \lesssim 4$, and found no evidence of a fixed point beside the O(8) FP that occurs in the model with $v_0 = 0$.

- Subsequent analyses [60], however, found an additional stable fixed point outside this region (point S in Fig. 1), located at $u^* \approx -3.4$ and $v^* \approx 5.3$.
- [74] The errors reflect the stability of the results of the different resummations with respect to the parameters b and α (see Ref. [72]) and the number of perturbative terms considered. They are obtained by considering how the estimates change when b and α vary within a reasonably large region around their optimal values (see Ref. [71] for a detailed description of the approach) and when the resummation is applied to the perturbative series with five (MZM scheme) or four ($\overline{\text{MS}}$ scheme) terms.
- [75] B. I. Halperin, T. C. Lubensky, and S. K. Ma, Phys. Rev. Lett. **32**, 292 (1974).
- [76] K. Kajantie, M. Karjalainen, M. Laine, and J. Peisa, Phys. Rev. B **57**, 3011 (1998).
- [77] S. Mo, J. Hove, and A. Sudbø, Phys. Rev. B **65**, 104501 (2002).
- [78] C. W. Garland and G. Nounesis, Phys. Rev. E **49**, 2964 (1994).
- [79] M. De Prato, A. Pelissetto, and E. Vicari, Phys. Rev. B **70**, 214519 (2004).
- [80] J. Berges and C. Wetterich, Nucl. Phys. B **487**, 675 (1997).
- [81] K. Fukushima, K. Kamikado, and B. Klein, Phys. Rev. D **83**, 116005 (2011).
- [82] S. Chandrasekharan and A. C. Mehta, Phys. Rev. Lett. **99**, 142004 (2007).
- [83] The estimate of the crossover exponent can be inferred from the results of Ref. [94].
- [84] B. Lucini, M. Teper, and U. Wenger, J. High Energy Phys. **01**, 061 (2004).
- [85] B. Lucini, A. Rago, and E. Rinaldi, Phys. Lett. B **712**, 279 (2012).
- [86] G. 't Hooft, Nucl. Phys. B **72**, 461 (1974).
- [87] L. McLerran and R. D. Pisarski, Nucl. Phys. A **796**, 83 (2007).
- [88] B. Lucini and M. Panero, Phys. Rep. **526**, 93 (2013).
- [89] Y. Hidata and N. Tamamoto, Phys. Rev. Lett. **108**, 121601 (2012).
- [90] F. Karsch and M. Lütgemeier, Nucl. Phys. B **550**, 449 (1999).
- [91] J. Engels, S. Holtmann, and T. Schulze, Nucl. Phys. B **724**, 357 (2005).
- [92] E. Witten, Nucl. Phys. B **156**, 269 (1979).
- [93] We use a different normalization with respect to Ref. [69]: the quartic couplings we use differ by a multiplicative factor of two from those of Ref. [69].
- [94] P. Calabrese, A. Pelissetto, and E. Vicari, Nucl. Phys. B **709**, 550 (2005).